Digest 2016, December 2016, 2013-2037

Liquefaction Behavior and Post-Liquefaction Volumetric Strain Properties of Low Plasticity Silt Sand Mixtures †

Eyyüb KARAKAN[1]
Selim ALTUN[2]

ABSTRACT

In this paper, the liquefaction behavior of silt-sand mixtures and post-liquefaction volumetric deformation properties were investigated. The study was performed on silt sand mixtures which were obtained during a foundation excavation in Bayraklı region of Izmir city in Turkey. In the study, undrained cyclic triaxial tests were conducted on samples having 8 different silt contents (0, 5, 10, 20, 40, 60, 80, 100%) in conformity with JGS 0542-2000 standard in order to reveal the effect of silt content on the liquefaction resistance of the samples. At the end of tests, output water amounts were measured with the help of a burette by opening the drainage valves in order to determine the volumetric deformation properties of the samples. In the liquefaction experiments, along with the increased silt contents the liquefaction criteria were determined by the void ratio concept between the coarse and fine grains instead of the relative density concept. With this perspective, threshold silt content in the liquefaction resistance of silt sand mixtures was also determined. The post-liquefaction volumetric deformation behavior of the samples was interpreted depending on the silt content.

Keywords: *Silt sand mixtures, liquefaction, volumetric deformation, intergranular - interfine void ratios.*

1. INTRODUCTION

Even the behavior of clean sands under cyclic loading has been investigated extensively for fifty years, an interest has risen on the cyclic behavior of soils with fines, especially silty sands, in the last two decades. The literature on the liquefaction phenomenon indicated that this type of soil was highly susceptible to liquefaction compared to clean sand. However, the results published in the literature concerning the effect of fines content on the liquefaction resistance of silty sands are still contradictory. Among the studies which were conducted in the field considering the liquefaction potential of sands with fines, it was seen that the presence of fines increased the liquefaction resistance [1, 2]. On the opposite side, the results of laboratory experiments indicated that a different tendency was shown when fines content was lower than 30% [3, 4]. While Koester [4] claimed that the liquefaction

1 Kilis 7 Aralık University, Kilis, Turkey - eyyubkarakan@gmail.com
2 Ege University, İzmir, Turkey - sealtun@gmail.com

† Published in Teknik Dergi Vol. 27, No. 4 October 2016, pp: 7593-7617

behavior was affected more significantly by the fines content rather than the plasticity index of the soil, Ishihara [5] and Prakash and Guo [6] reported that the fine grained soils with high plasticity may be less susceptible to liquefaction. Finn et al. [7] remarked that researchers achieved varying results while investigating the effect of fines content on the liquefaction resistance as different criteria were accepted by them.

The effect of fines content on the liquefaction resistance depends on the particle diameter. The results of laboratory experiments showed that the voids between the sand particles had no effect on the soil resistance in the soils with fines content less than 30%. This result decreases the global void ratio (e_0). Therefore, liquefaction resistance decreases in the soils at the same global void ratio with the increment of fines content and the sand skeleton (e_{SK}) at different intergranular void ratios shows more dominant behavior [8, 9, 10, 11]. In the same way, if the fine particles are more dominant in the sand matrix then general behavior largely depends on the fines content. Amini and Qi [12] stated that the cyclic resistances of silty sand mixtures steadily increased as the fines content increased but Belkhatir et al. [13] and Stamatopoulos [14] stated that the cyclic resistances of silty sand mixtures would decrease along with the increase of fines content. On the other side, Koester [4]; Papadopoulou and Tika, [15]; Polito and Martin, [8]; Xenaki and Athanasopoulos, [16] observed that the increase of fines content first decreased and then increased the cyclic resistances of silty sand mixtures up to a threshold fines content value.

In the silty sand mixtures, the threshold silt content value is a significant parameter which determines the transition from sand to silt. This threshold value varies depending on the sand type, fines type and the global void ratio. Therefore, the effect of silt content on liquefaction resistance of silt sand mixtures may yield to different results if the global void ratio is used. Especially, Troncoso [4] determined that the liquefaction resistance decreased as the fines content increased up to 30%. On the other side, Xenaki and Athanasopoulos [16] concluded that critical fines content was 44%. In the results of work reported by Polito [17], it was shown that the threshold silt content value of non-plastic silt sand mixtures was between of $25<FC_{th}<45$ where FC_{th} denotes the threshold value of silt content.

The effect of fines content is a significant parameter on the behavior of silt sand mixtures under cyclic loadings. However, there is a controversy on the published literature concerning the effect of fines content on the liquefaction of soils. If the fines content is remarkably low, the fines in the soil matrix remain passive and float in the voids. Therefore, using new index parameters such as intergranular and interfine void ratios are very significant in terms of assessing the shear strength of silt sand mixtures [9, 18]. Consequently, there is a need for estimating the effect of two sub-matrices namely as coarse and fine matrices on the strain transformation behavior of silt sand mixtures.

The main objective of this study is to determine the effect of fines content on the dynamic behavior of natural silty sand collected from a foundation excavation in Bayraklı (Izmir, Turkey) and to evaluate the role of intergranular-interfine void ratios in the liquefaction resistance of silt sand mixtures. The second objective of this study is to reveal the volumetric deformation properties of silt sand mixtures considering the silt content of the mixture by measuring the volume of water collected in the burette at the end of dynamic cyclic triaxial tests. The results of undrained cyclic triaxial compression tests conducted on the silt sand mixtures with various fines content were presented and discussed within this scope.

1.1. Threshold Fines Content Ratio

As it is well known, the soil behavior is manipulated by the skeleton of sand grains if the fines content is under a specific percentage. In this case, the fine particles are passive and they have no contribution to the shear resistance of the soil matrix. When the fine particles exceed a limiting value, the fine grains dominate the soil behavior and in this case, the sand grains are accepted as the void. This limiting value is called the ''threshold fines content'' (FC_{th}) (Figure 1). There are two different definitions in literature on the threshold fines content. The first one of them is the ''fines content'' which was suggested by Polito and Martin [8] and called the maximum fines content in the voids by keeping a fixed sand skeleton. Another term was used by Yang et al. [19] and it is defined as the fines content which transforms the peak resistance of soil from positive to negative.

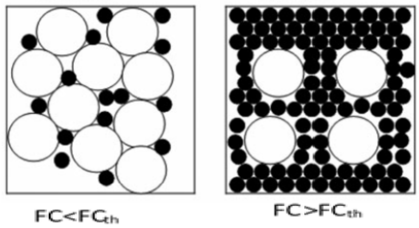

Figure 1. Two soil matrixes with fine grains

1.2. Intergranular– Interfine Void Ratio Concepts

The concept of intergranular void ratio suggested by Kuerbis et al. [20] may be first defined as the fine particles simply filling the void between the coarse particles by accepting the fines content as the volumetric void. Dash and Sitharam [21]; Kuerbis et al. [20]; Polito and Martin [8] named the intergranular void ratio as the sand skeleton void ratio and Dasari et al. [22] described it as the granular void ratio. The intergranular void ratio may be easily calculated with the formula suggested by Thevayanagam [9] by assuming that the specific gravity of coarse particles are equal to the specific gravity of fine particles;

$$e_g = \frac{e+f_c}{1-f_c} \tag{1}$$

Here, e corresponds to the global void ratio, e_g corresponds to the intergranular void ratio and f_c corresponds to the fines content (f_c=FC/100).

In literature, various researchers stated that the cyclic resistances of soils increased along with the increase of fines content at the same intergranular void ratio [14, 15, 16, 20]. Polito and Martin [8] tested two different sands from Monterey and Yasteville and observed that for a given intergranular void ratio and with the increment of fines content the cyclic resistance of Monterey sand remained stable while the cyclic resistance of Yasteville sand slightly increased.

The second explanation may be defined as the interfine void ratio. The sand grains are accepted to exist separated from the mixture if they contain a high amount of fine particles and in this case, the interfine void ratio may be used as a parameter.

$$e_f = \frac{e}{f_c} \tag{2}$$

2. TESTING PROCEDURE

2.1. Materials Used

The soil used in this study was brought from a construction site in Bayraklı (Izmir, Turkey). The natural soil was classified as SM in accordance with the Unified Soil Classification System. Eight different variations of silt-sand mixtures were obtained by sieving the soil passing through sieves No. 4 and No. 200. The soil finer than 74 microns (No. 200) were separated from the virgin soil in order to create different combinations of silt-sand mixtures. The sand size particles consisted both angular and rounded grains. The uniformity coefficient of sand was C_u=4.22 and the effective grain size was D_{50}=0.24 mm. The maximum and minimum void ratios of the sand were 0.941 and 0.664, respectively. The separated silt part of the soil had a liquid limit of w_L=40 and its plasticity index was I_p=13. The specific density of sand and silt were both Gs=2.7. The sand and silt were mixed in order to obtain mixtures with different silt contents in the order of 0%, 5%, 10%, 20%, 40%, 60%, 80% and 100%. The grain size distributions of sand and silt are shown in Figure 2. The silt content of natural soil (SM) obtained from the excavation was only 20%.

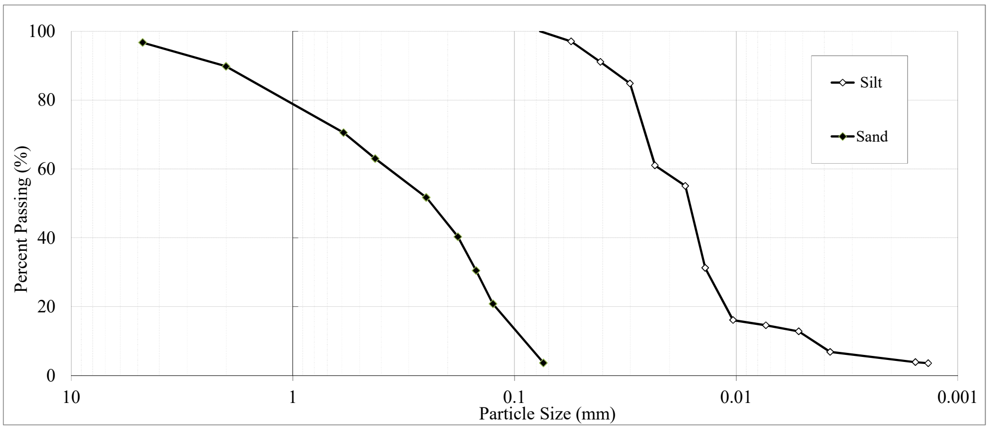

Figure 2. Grain Size Distribution

In order to determine the maximum and minimum void ratios of silt-sand mixtures, ASTM D4253/4254 procedure were used. The measurements were repeated three times for each mixture. The variation of maximum and minimum void ratios with increasing silt content are shown in Figure 3. When fine particles in the mixture increased up to a specific value, first the void ratios showed a tendency to decrease, but when this value was exceeded the void ratios were increased. There is no information that leads to determining maximum and minimum void ratios for soils with fines content more than 15%. ASTM 4254-91 and ASTM-4253-93 standards are relevant for the materials with a maximum fines content of 15% . However, it is seen that same procedures are applied as in ASTM standards in order to determine maximum and minimum void ratios in the soils with fines content more than 15% [9, 12, 14, 16].

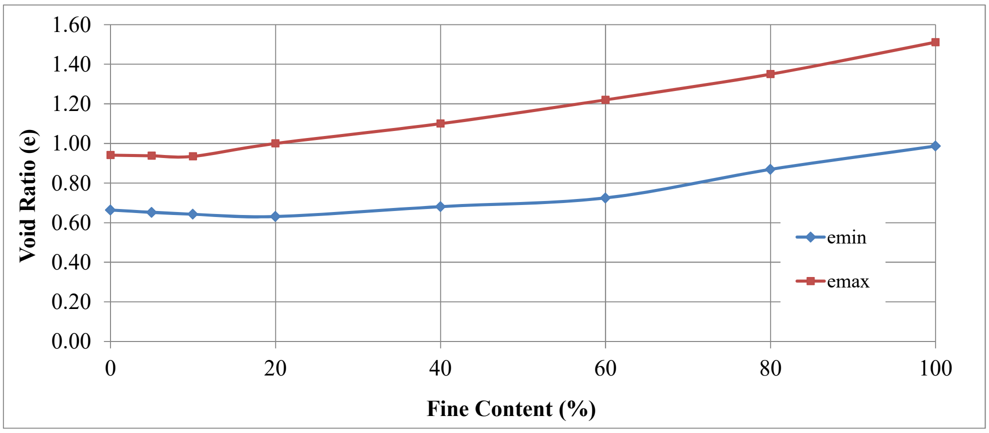

Figure 3. Maximum and minimum void ratios varying with the silt content of the mixtures

2.2. Dynamic Triaxial Compression Test System

In order to search for the stress-strain parameters of silty sands on the dynamic behavior, 58 dynamic triaxial compression tests were conducted on four sets. The properties of silt-sand mixtures, testing conditions and the dynamic testing results obtained by using intergranular and interfine void ratio concepts are summarized in Table 1. As an addition to the routine experiment program, some randomized experiments were repeated in order to control the accuracy of results of sample preparation at the same void ratio and under the same loading conditions. The experiments were conducted on the samples which had 50 mm diameter and 100 mm height. All samples were prepared with the method of dry deposition. Also, all samples were consolidated under effective confining stress of 100 kPa.

The experiments were conducted under strain controlled conditions by using a full automatic dynamic triaxial compression testing system belonging to Seiken. The samples were prepared in conformity with JGS 0520-2000 standard and the dynamic traxial testing was conducted in conformity with JGS 0541-2000 standard. CO_2 was passed through the samples as a first step in order to ensure the saturation and then flowing water was passed through the entire sample. Afterwards, a back pressure was applied and Skempton B value was obtained and this value is confirmed to be higher than 0.96 in all experiments. The samples were isotropically consolidated under an effective confining stress of 100 kPa and then cyclic loadings were applied in a stress controlled manner under undrained conditions.

Table 1. Properties of silt sand mixtures and their dynamic testing results

Test No	Specimen Dimensions		Fine Content	Void Ratio	Intergranular	Interfine	Maximum	Minimum	Pore Pressure	Cell Pressure	Back Pressure	CSR	Number of Cycles
	D(mm)	H(mm)	(%)	e	es	ef	e_max	e_min	Coefficient, B	(kPa)	(kPa)		N
1	50	99	0	0.858	0.858		0.941	0.664	0.997	275	175	0.156	30
2	48.52	99.76	0	0.858	0.858		0.941	0.664	1	180	80	0.222	2.5
3	49.18	99.11	0	0.858	0.858		0.941	0.664	1	200	100	0.187	10.5
4	49.59	99	0	0.858	0.858		0.941	0.664	0.97	270	170	0.133	103
5	49.32	99.18	0	0.858	0.858		0.941	0.664	1	280	180	0.105	29
6	49.7	99.09	5	0.852	0.95		0.938	0.652	1	225	125	0.226	5
7	50	98.89	5	0.852	0.95		0.938	0.652	0.96	360	260	0.246	2.5
8	49.96	98.98	5	0.852	0.95		0.938	0.652	0.987	250	150	0.127	76.5
9	49.92	99	5	0.852	0.95		0.938	0.652	0.982	250	150	0.172	15.5
10	49.44	99.1	5	0.852	0.95		0.938	0.652	1	175	75	0.102	425
11	50	98.88	10	0.847	1.053		0.935	0.643	0.965	300	200	0.258	1.5
12	49.84	98.88	10	0.847	1.053		0.935	0.643	0.977	225	125	0.209	3.5
13	49.56	98.98	10	0.847	1.053		0.935	0.643	0.983	175	75	0.185	10.5
14	49.67	98.97	10	0.847	1.053		0.935	0.643	0.984	200	100	0.141	53
15	49.88	99.01	20	0.889	1.362		1	0.631	0.993	275	175	0.140	38.5
16	50	99	20	0.889	1.362		1	0.631	0.997	300	200	0.111	199
17	49.7	98.91	20	0.889	1.362		1	0.631	1	275	175	0.167	15
18	49.48	98.96	20	0.889	1.362		1	0.631	1	175	75	0.197	6.5
19	49.57	98.8	40	0.974	2.291		1.1	0.681	1	250	150	0.130	38.5
20	49.52	98.78	40	0.974	2.291		1.1	0.681	1	250	150	0.108	241
21	49.52	98.78	40	0.974	2.291		1.1	0.681	1	275	175	0.163	14.5
22	49.57	98.77	40	0.974	2.291		1.1	0.681	1	250	150	0.187	4.5
23	49.54	98.71	60	1.072		1.786	1.22	0.725	1	225	125	0.142	28.5
24	49.53	98.65	60	1.072		1.786	1.22	0.725	1	225	125	0.114	95.5
25	49.39	98.41	60	1.072		1.786	1.22	0.725	1	200	100	0.171	7.5
26	49.75	98.56	60	1.072		1.786	1.22	0.725	1	275	175	0.197	3.5
27	49.52	98.14	80	1.206		1.507	1.35	0.869	1	250	150	0.131	17.5
28	49.35	98.23	80	1.206		1.507	1.35	0.869	1	175	75	0.112	163
29	49.33	98.45	80	1.206		1.507	1.35	0.869	1	175	75	0.197	2.5
30	49.78	98.22	80	1.206		1.507	1.35	0.869	1	225	125	0.125	73.5
31	49.63	98.26	100	1.354		1.354	1.511	0.987	1	225	125	0.156	13.5
32	49.5	98.45	100	1.354		1.354	1.511	0.987	1	175	75	0.105	163.5
33	49.47	98.94	100	1.354		1.354	1.511	0.987	0.985	375	275	0.133	35.5
34	49.42	98.47	100	1.354		1.354	1.511	0.987	1	200	100	0.198	4.5
35	49.92	99.44	0	0.803	0.803		0.941	0.664	0.981	225	125	0.208	19
36	50	99.34	0	0.803	0.803		0.941	0.664	0.973	400	300	0.255	6
37	49.71	99.42	0	0.803	0.803		0.941	0.664	0.978	200	100	0.162	151
38	49.64	99.38	0	0.803	0.803		0.941	0.664	0.995	200	100	0.327	2.5
39	50	99.12	20	0.816	1.269		1	0.631	0.978	275	175	0.273	2.7
40	49.52	99.21	20	0.816	1.269		1	0.631	1	175	75	0.209	7
41	49.53	99.2	20	0.816	1.269		1	0.631	1	175	75	0.163	32
42	49.6	99.22	20	0.816	1.269		1	0.631	1	200	100	0.136	126.5
43	49.7	99.12	40	0.891	2.151		1.1	0.681	0.992	225	125	0.274	1.5
44	49.52	99.08	40	0.891	2.151		1.1	0.681	0.995	175	75	0.221	5
45	49.92	98.97	40	0.891	2.151		1.1	0.681	1	250	150	0.163	35
46	49.55	99.15	40	0.891	2.151		1.1	0.681	1	175	75	0.137	95
47	49.6	98.78	60	0.973		1.621	1.22	0.725	1	175	75	0.279	0.5
48	49.58	99.07	60	0.973		1.621	1.22	0.725	1	180	80	0.225	3.5
49	49.55	99.02	60	0.973		1.621	1.22	0.725	0.995	175	75	0.164	29.5
50	49.51	99.02	60	0.973		1.621	1.22	0.725	0.992	175	75	0.124	423
51	49.95	98.77	80	1.11		1.387	1.35	0.869	0.987	250	150	0.265	0.5
52	49.72	98.79	80	1.11		1.387	1.35	0.869	0.995	250	150	0.210	4
53	49.69	98.85	80	1.11		1.387	1.35	0.869	0.992	225	125	0.164	26
54	49.54	98.86	80	1.11		1.387	1.35	0.869	1	200	100	0.140	61
55	49.4	98.79	100	1.249		1.249	1.511	0.987	1	175	75	0.138	132
56	49.41	98.81	100	1.249		1.249	1.511	0.987	1	175	75	0.210	5.5
57	49.48	98.99	100	1.249		1.249	1.511	0.987	1	175	75	0.169	30
58	49.82	989.71	100	1.249		1.249	1.511	0.987	0.992	250	150	0.265	0.5

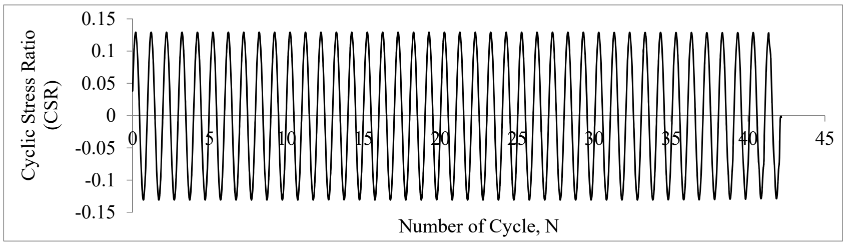

(a)

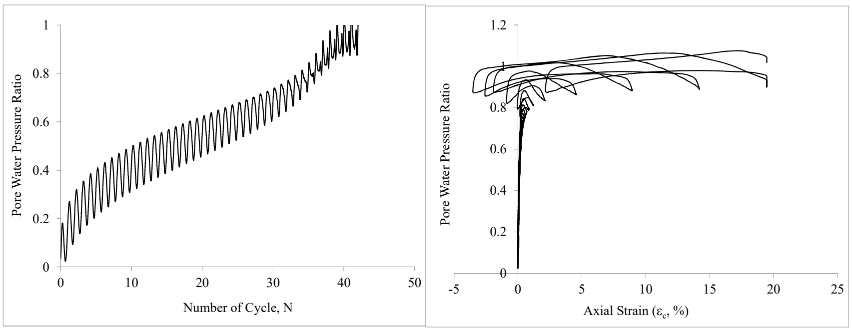

(b)

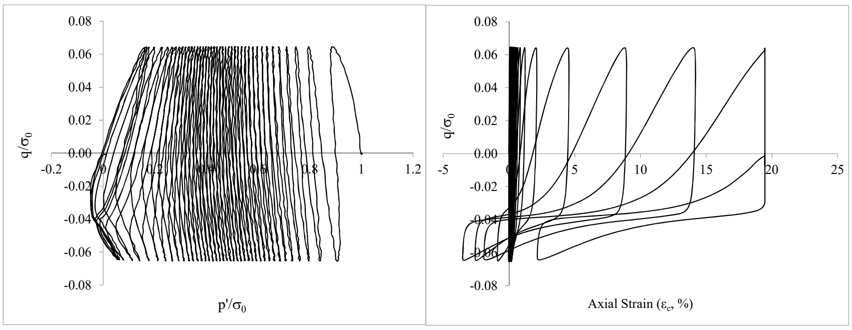

(c)

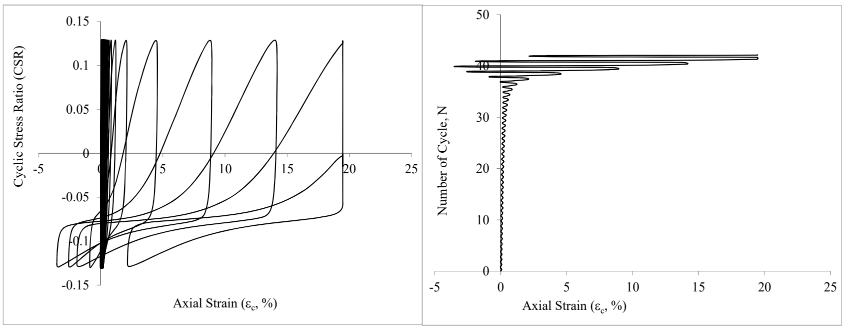

(d)

Figure 4. The relationship of
a) CSR- Number of cycles; b) Pore water pressure ratio and number of cycles; c) q/σ_0' - axial strain; d) CSR - axial strain

The cyclic loadings were recorded continuously and excess pore water pressure, cyclic axial strain and cyclic stress ratio were obtained for each sample. Two criteria are taken in to account in JGS 0542-2000 standard in order to define the liquefaction stage. If the amplitude of cyclic loading is high, the number of cycles to attain liquefaction is accepted as the maximum excess pore water pressure required in order to reach to 95% of effective confining stress otherwise, the number of cycles to liquefaction is determined when 5% of double amplitude of axial strain was achieved in the sample. Typical test results which were obtained from a dynamic triaxial compression test conducted on silt-sand mixture is shown in Figure 4 (a)-(d). The cyclic deviator stress ratio applied to the sample versus the number of cycles is shown in Figure 4a. 42 cycles which involved a continuous sequence of compression and expansion were continuously applied to simulate dynamic conditions. The severity of cyclic loading was changed in order to be able to produce different cyclic stress ratios (CSR) and their corresponding number of cycles to liquefaction. In this study, the number of cycles applied varied between 1 and 1000 cycles. In Figure 4b, the variation of pore water pressure ratio with the number of cycles and the variation of the pore water pressure ratio with axial strain are shown. The pore water pressure ratio had continuously increased with the number of cycles applied to the samples. In Figure 4b, the rate of normalized stress are at the pressure side due to that cyclic axial strain was positive (Figure 4c). The normalized stress path is shown in Figure 4c. While the cyclic stress ratio applied corresponded to low deformation levels, the samples maintained their stability after that the soil liquefied along with the increased number of cycles under enlarged deformations. After 35 cycles, the pore water pressure ratio reached to 90% and after this point the cyclic axial strain changed considerably (Figure 4d).

3. DYNAMIC TRIAXIAL COMPRESSION TEST RESULTS

3.1. Liquefaction Behavior of Silt Sand Mixtures Under Undrained Cyclic Loading Condition

In this part, the effect of silt content, global void ratio concept, intergranular-interfine void ratio concepts on the liquefaction resistance of the silt sand mixtures are discussed. In order to understand the effect of void ratio depending on the cyclic axial strain ratio (CSR), a large number of dynamic triaxial tests were conducted. In this paper, the liquefaction resistances of silt sand mixtures are shown in Figure 5 as CSR-N curves. Figure 5 shows the effect of silt content on the liquefaction resistances of silt sand mixtures for a constant value of global void ratio. It was seen that the liquefaction resistance decreased along with the increase of silt content up to 40% in the silt sand mixtures with low plasticity for a constant value of global void ratio. This value is defined as the threshold silt content (FC_{th}). If the silt content is above 40%, the tendency becomes reversed and the liquefaction resistance increases (Figure 5a, 5b).

It was determined that the liquefaction resistance decreased in the low plasticity silty sands along with the increase of silt content up to 40% for the a stable value of global void ratio. After this critical value the framework offered by Tevayanagam [9] contradicts with the threshold value, this tendency reverse and the liquefaction resistance increases as the silt content increases. The cyclic stress ratios (CSR_{20}) corresponding to 20 cycles of loading are obtained from Figure 5&6 for the samples which had different silt contents and consolidated under a stress of 100 kPa. In this paper, CSR_{20} value is defined as the cyclic stress ratio at which double amplitude of axial strain at 20 cycles is 5%. In Figure 6, it is clearly seen that the critical silt content is 40%. The critical silt content is a key value that separates the increment and decrement of liquefaction resistance.

The effect of silt content on the liquefaction resistance of silt sand mixtures for intergranular and interfine void ratios are shown in Figure 7. For the silt contents below the threshold value, it is clearly seen that the increase of silt content decreased CSR_{20} value. In Figure 7, there is a different tendency concerning the effect of silt content on the liquefaction resistance of silt sand mixtures in terms of the effect of interfine void ratio. In this case, the increase in the silt content decreases CSR_{20} value under the same conditions ($FC>FC_{th}$).

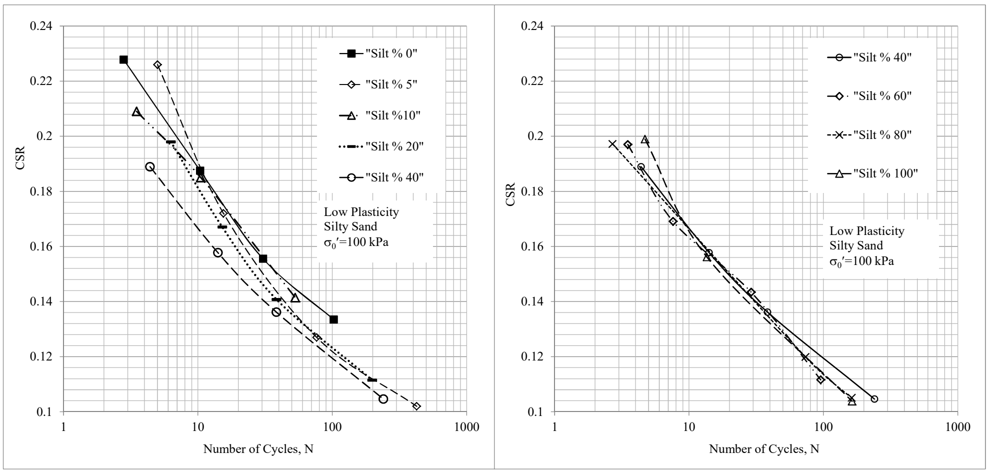

(a) *(b)*

Figure 5. The effect of silt content on liquefaction resistance in the silt sand mixtures with low plasticity
(a)0<FC<40 (b) 40<FC<100 (σ_0'=100kPa)

In other words, CSR_{20} value corresponding to 20 cycles decreases but the intergranular void ratio increases if the silt content increases when the silt content is lower than the threshold silt content ($FC<FC_{th}$) as shown in Figure 7. On the other side, CSR_{20} value corresponding to 20 cycles and interfine void ratio decreases if the silt content increases when the silt content is higher than the threshold silt content ($FC>FC_{th}$). In Figure 8, the change of silt content corresponding to intergranular and interfine void ratios are shown. It is seen that interfine void ratio decreases as the silt content increases and on the other hand the intergranular void ratio increases along with the increment of silt content. 40% silt content is the intersection of both void ratios and it is defined as the threshold silt content.

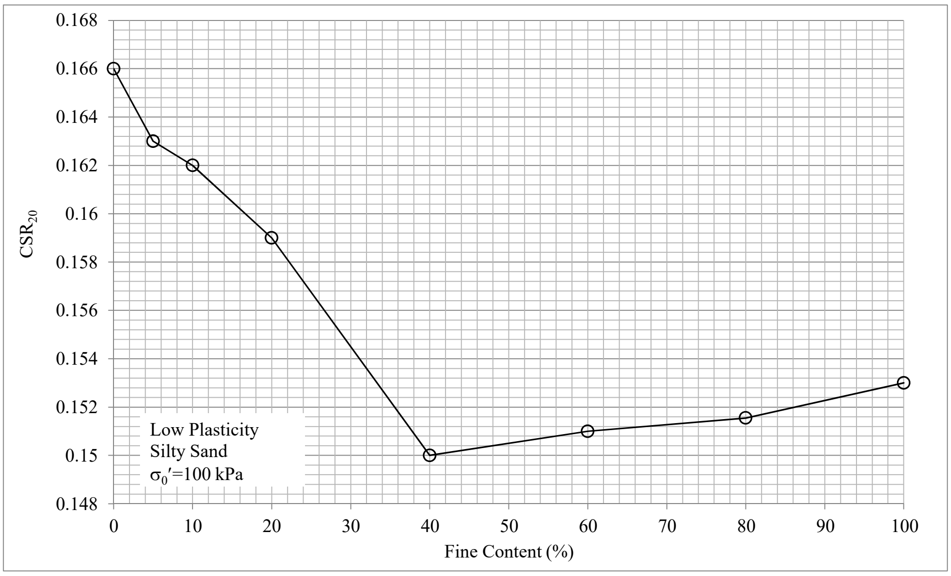

Figure 6. CSR_{20} and the effect of Silt content in the silt-sand mixtures with low plasticity

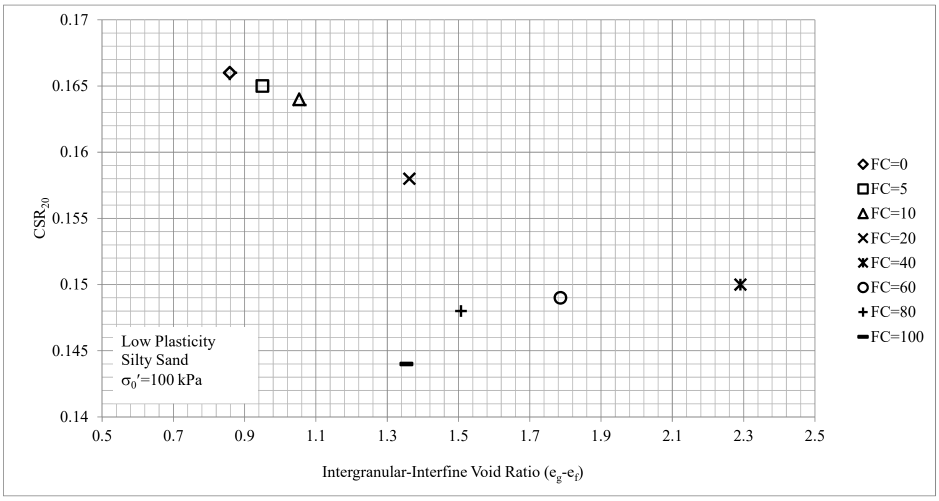

Figure 7. CSR_{20}-Intergranular- interfine void ratio variation on the liquefaction behavior of silt sand mixtures with low plasticity

For different silt contents, the resistance of silt sand mixtures to liquefaction with different global void ratios is shown in Figure 9. The cyclic stress ratio corresponding to 20 cycles is defined as the liquefaction resistance. In Figure 9, the increase in global void ratio showed that the resistance to the liquefaction decreased in silt sand mixtures. It is seen that the curve in figure 9 is the most appropriate curve obtained from the experimental data in the silt sand mixtures to determine CSR_{20} values. For a constant void ratio value e, interfine void ratio value, e_f, decreases and intergranular void ratio value, e_g, increases as, the silt content increases . If the silt content is lower than the threshold silt content ($FC<FC_{th}$), the behavior of silt sand mixtures is controlled by the sand particles and their liquefaction resistance decrease as the effects of fine particles to the intergranular contact will be limited. If the silt content is higher than the threshold value, the coarse particles only reinforce the matrix and the effect of interfine void ratio becomes significant (Figure 7 and Figure 8).

The correlation of cyclic stress ratio (CSR) at a constant void ratio and the number of cycles for various silt contents is shown in Figure 10. It is observed that the cyclic stress ratio decreased for FC=0% at a specific number of cycles when the effective confining stress increases from 50 kPa to 150 kPa. These results are in conformity with literature [15, 17]. The effect of silt content between cyclic stress ratio and number of cycles at constant void ratios are shown in Figure 11.The cyclic stress ratio (CSR) increases with the silt content up to the threshold value and after the threshold is exceeded the cyclic stress ratio (CSR) decreases for a given number of cycles.

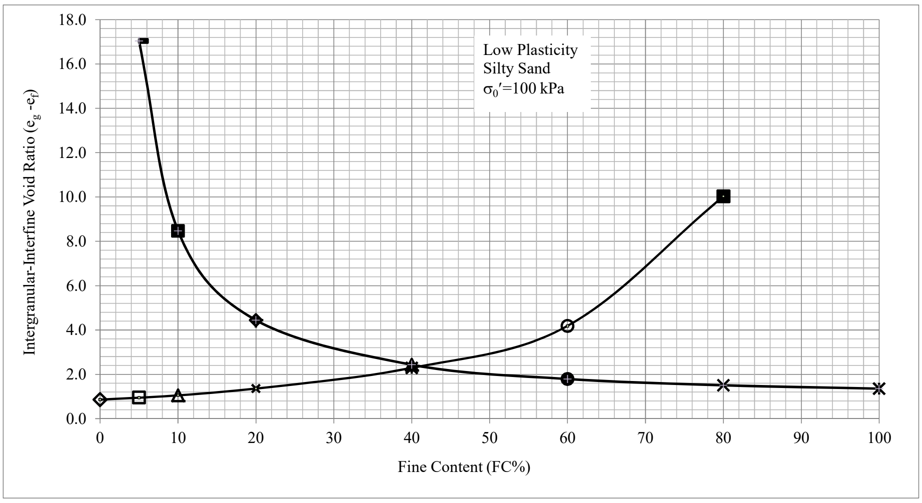

Figure 8. Threshold silt content for intergranular-interfine void ratios silt sand mixtures with low plasticity

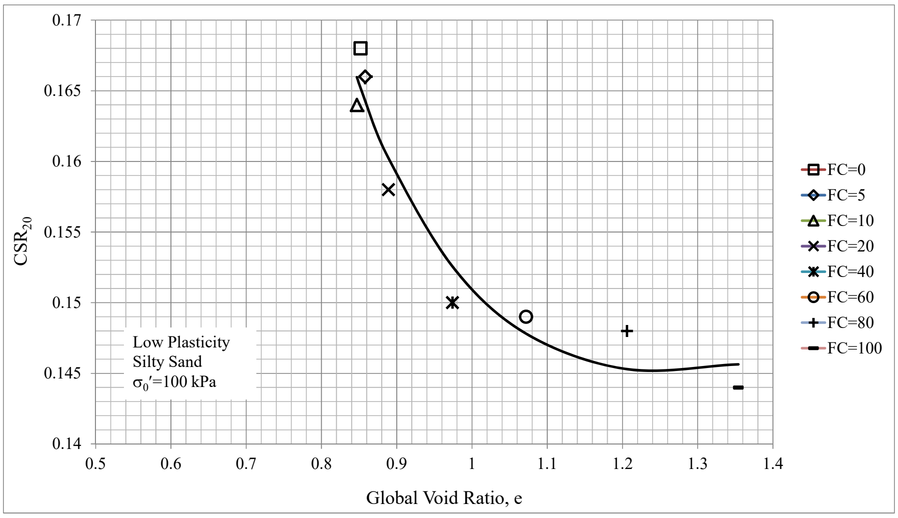

Figure 9. CSR_{20} – global void ratio relation in silt sand mixtures with low plasticity

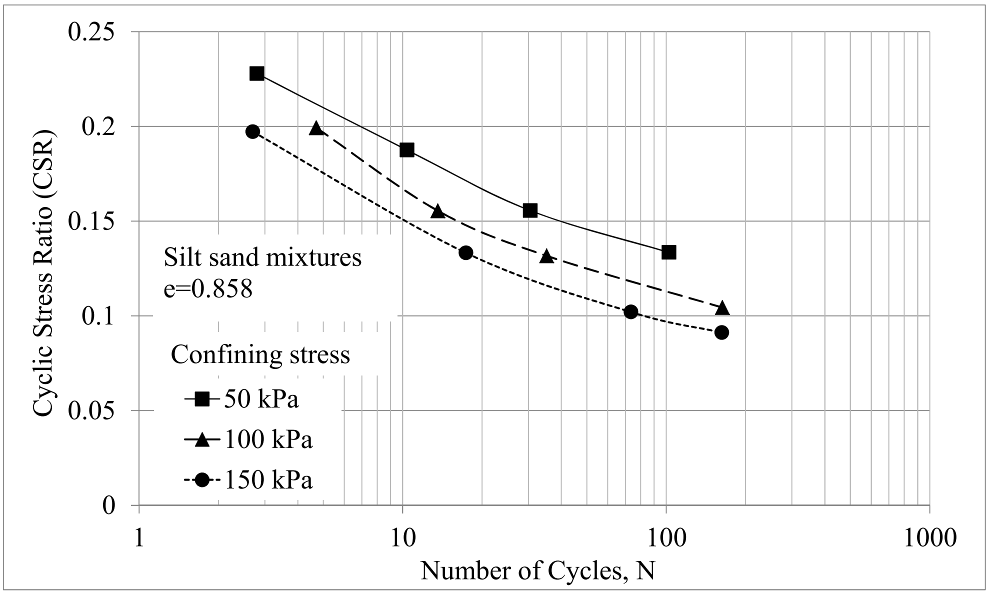

Figure 10. The relation between CSR and the number of cycles in silt sand mixtures with a constant global void ratio considering the effect of confining stress

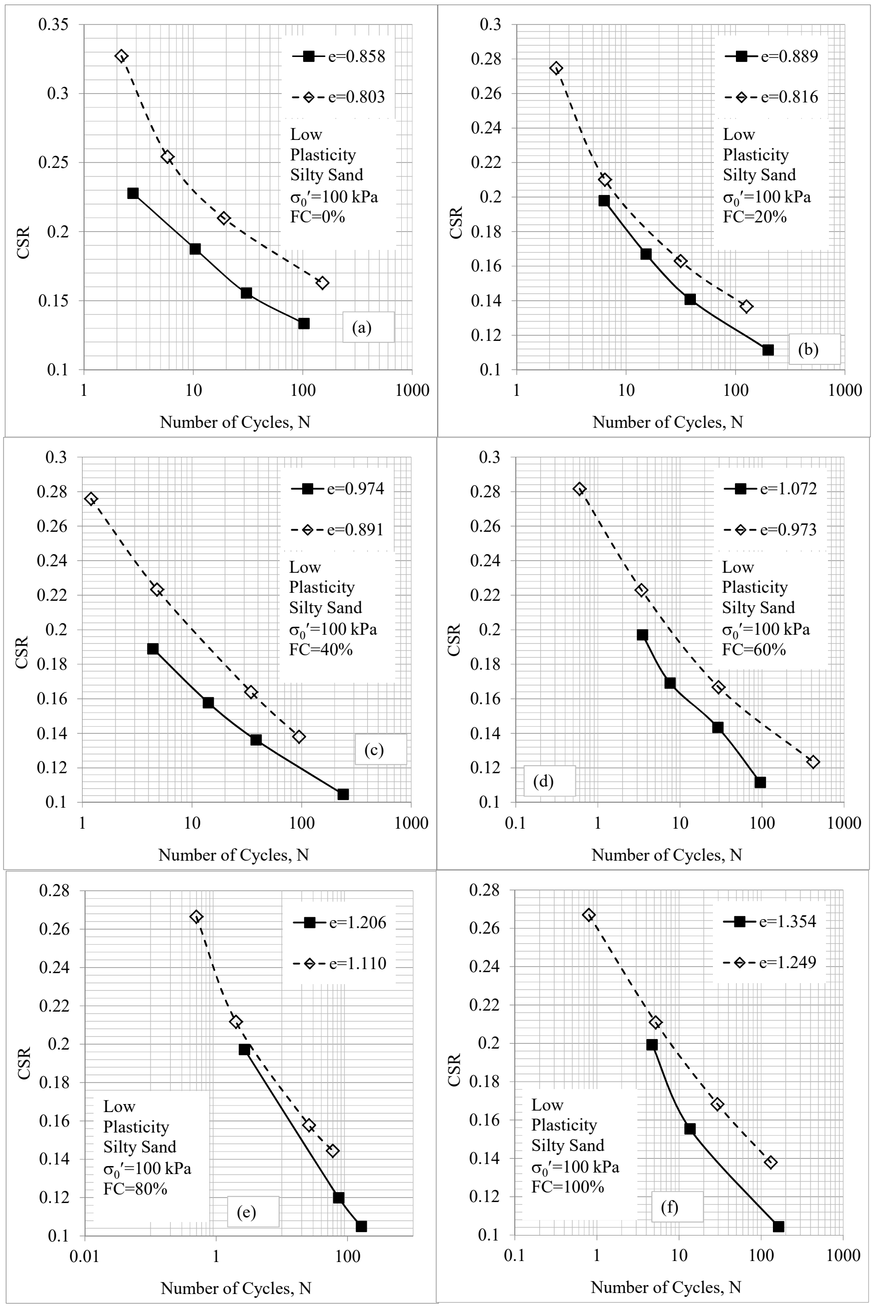

Figure 11. The effect of silt content in the relation between CSR and the number of cycles in silt sand mixtures with constant void ratios

3.2. Volumetric Change in Reconsolidation Process Following Undrained Cyclic Loading

It is known that the sands exposed to earthquake loads shows contractive behavior. The consolidation of soil after the earthquake reveals itself as the total and differential settlement on the ground surface. The settlements which occurred due to the earthquakes lead to substantial damages on the structures with shallow foundations and lifelines. Dry sandy soils consolidate quickly and therefore the settlement occurs immediately at the end of earthquake. The settlement of saturated sandy soils takes longer time depending on the existence of fine particles. In these soils, the settlement occurs along with the dissipation of excess pore water pressure due to the earthquake. The dissipation of excess pore water pressure depends on the parameters such as the fines content, relative density of soil, drainage length and effective confining stress.

Lee and Albaisa [23], Tatsuoka et al. [24] and Ishihara et al. [25] conducted dynamic triaxial compression tests on sand soils and investigated the volumetric change occurring due to the formation of excess pore water pressure. It was shown that the post-liquefaction volumetric strain in the soils did not only affect the unit weights of soils but also it affected the maximum shear strain which occurred along the cyclic loadings in the dynamic triaxial compression tests. Based on this knowledge, Tokimatsu and Seed [26] developed a method to estimate the post-liquefaction settlements. Ishihara and Yoshimine [27] developed a method for the estimation of settlements on the soil surface depending on the safety factor by taking maximum shear strain as the basic parameter alternating the post-liquefaction volumetric strain.

Several tests were performed to determine the volumetric change of sands as a result of cyclic shear strains under undrained conditions along the distribution of pore water pressure development. The silt sand mixtures with varying silt contents were isotropically consolidated under 100 kPa effective confining stress and they were subjected to shear strains under strain controlled and undrained conditions The experimental conditions, loading conditions, shear stress and volumetric strain values are shown in Table 2. The volumetric changes of strain was measured by opening drain valves for the dissipation of pore water pressure which developed after the completion of loading in undrained conditions. The volumetric change of strain was correlated with the settlement characteristics of liquefied soils after dynamic loading.

Along the reconsolidation process, maximum amplitude of shear strain, γ_{mak}, were graphed with, ε_v, volumetric strain. Dynamic triaxial compression tests were conducted on silt sand mixtures with low plasticity where two different relative densities and eight different silt contents were available. The curves obtained according to the relative densities of 25% and 50% are shown in Figures 12 and 13, respectively.

The experiments were conducted for two different relative densities (Dr=25% and Dr=50%) and the variation of maximum amplitude of shear strain with the volumetric strain is shown for the samples having different fines content. Here, it was seen that the volumetric strains increased as the fines content increased for a constant maximum amplitude of shear strain. In literature, Tatsuoka et al. [28], Sasaki et al. [29], and Kokusho et al. [30] also showed that the volumetric strain value increased and the relative density decreased for clean sands as a result of dynamic triaxial and torsional shear tests.

Table 2. Post-liquefaction volumetric strain and factor of safety values

Test No	Silt Content (%)	Cyclic Stress (kPa)	Cyclic Stress Ratio (CSR)	Number of Cycle, N	Volumetric Strain (%)	Axial Strain $(\varepsilon a)_{sa}$ (%)	Cyclic Stress Ratio for 20 cycle	Factor of Safety F_l=CSR_{N20}/CSR	Shear Strain (%)
1	0	31.123	0.156	30	3.198	7.176	0.167	1.073	10.764
2	0	44.350	0.222	2.5	3.188	10.731	0.167	0.753	16.097
3	0	37.414	0.187	10.5	3.246	8.467	0.167	0.893	12.700
4	0	26.669	0.133	103	3.044	8.824	0.167	1.252	10.148
5	0	21.073	0.105	29	3.003	5.075	0.167	1.585	7.613
6	5	45.111	0.226	8	3.486	10.467	0.164	0.727	15.701
7	5	49.243	0.246	5	3.556	10.687	0.164	0.666	16.031
8	5	25.445	0.127	76.5	3.100	10.898	0.164	1.289	12.533
9	5	34.481	0.172	15.5	3.215	10.114	0.164	0.951	15.171
10	5	20.351	0.102	425	3.080	7.909	0.164	1.612	11.863
11	10	51.543	0.258	1.5	3.896	14.059	0.168	0.652	21.089
12	10	41.802	0.209	3.5	3.752	12.794	0.168	0.804	19.191
13	10	37.000	0.185	10.5	3.960	12.961	0.168	0.908	16.201
14	10	28.292	0.141	53	3.957	8.704	0.168	1.188	13.056
15	20	28.016	0.140	38.5	3.714	8.169	0.157	1.121	12.254
16	20	22.276	0.111	199	3.568	6.971	0.157	1.410	10.456
17	20	33.409	0.167	15	3.661	7.866	0.157	0.940	12.979
18	20	39.434	0.197	6.5	3.804	10.009	0.157	0.796	15.014
19	40	25.943	0.130	38.5	4.398	8.728	0.15	1.156	13.091
20	40	21.516	0.108	241	4.330	8.480	0.15	1.394	12.720
21	40	32.553	0.163	14.5	4.347	10.692	0.15	0.922	14.435
22	40	37.378	0.187	4.5	4.384	10.414	0.15	0.803	15.621
23	60	28.337	0.142	28.5	4.297	8.865	0.151	1.066	13.298
24	60	22.707	0.114	95.5	4.426	7.744	0.151	1.330	11.616
25	60	34.258	0.171	7.5	4.471	11.561	0.151	0.882	17.341
26	60	39.357	0.197	3.5	4.199	12.438	0.151	0.767	18.657
27	80	26.161	0.131	17.5	5.048	9.901	0.15	1.147	14.852
28	80	22.349	0.112	163	5.142	9.835	0.15	1.342	14.753
29	80	39.336	0.197	2.5	5.159	12.097	0.15	0.763	18.146
30	80	24.948	0.125	73.5	4.930	9.820	0.15	1.203	14.730
31	100	31.112	0.156	13.5	4.978	12.018	0.144	0.926	18.026
32	100	20.976	0.105	163.5	5.138	10.111	0.144	1.373	15.167
33	100	26.556	0.133	35.5	4.976	10.234	0.144	1.085	16.886
34	100	39.525	0.198	4.5	4.988	10.504	0.144	0.729	19.432
35	0	41.544	0.208	19	2.890	5.800	0.208	1.001	8.700
36	0	50.941	0.255	6	2.767	6.304	0.208	0.817	9.456
37	0	32.497	0.162	151	2.812	5.719	0.208	1.280	8.578
38	0	65.376	0.327	2.5	2.769	10.075	0.208	0.636	10.125
39	20	54.675	0.273	2.7	3.358	9.356	0.174	0.636	14.034
40	20	41.738	0.209	7	3.631	8.327	0.174	0.834	12.491
41	20	32.605	0.163	32	3.473	7.242	0.174	1.067	10.863
42	20	27.174	0.136	126.5	3.541	7.758	0.174	1.281	10.473
43	40	54.732	0.274	1.5	3.445	12.236	0.179	0.654	15.295
44	40	44.136	0.221	5	3.623	9.424	0.179	0.811	14.137
45	40	32.541	0.163	35	3.640	8.014	0.179	1.100	12.021
46	40	27.491	0.137	95	3.596	8.234	0.179	1.302	12.352
47	60	55.888	0.279	0.5	3.908	12.411	0.176	0.630	18.616
48	60	44.968	0.225	3.5	3.993	11.931	0.176	0.783	17.897
49	60	32.840	0.164	29.5	4.073	9.050	0.176	1.072	13.575
50	60	24.709	0.124	423	4.053	8.779	0.176	1.425	13.168
51	80	52.969	0.265	0.5	4.210	14.609	0.163	0.615	21.913
52	80	41.981	0.210	4	4.230	11.288	0.163	0.777	19.754
53	80	32.779	0.164	26	4.199	9.126	0.163	0.995	17.795
54	80	27.947	0.140	61	4.261	12.799	0.163	1.166	17.278
55	100	27.656	0.138	132	4.649	9.433	0.177	1.280	14.149
56	100	42.043	0.210	5.5	4.552	10.679	0.177	0.842	16.019
57	100	33.712	0.169	30	4.498	9.554	0.177	1.050	14.332
58	100	53.068	0.265	0.5	4.629	14.249	0.177	0.667	19.236

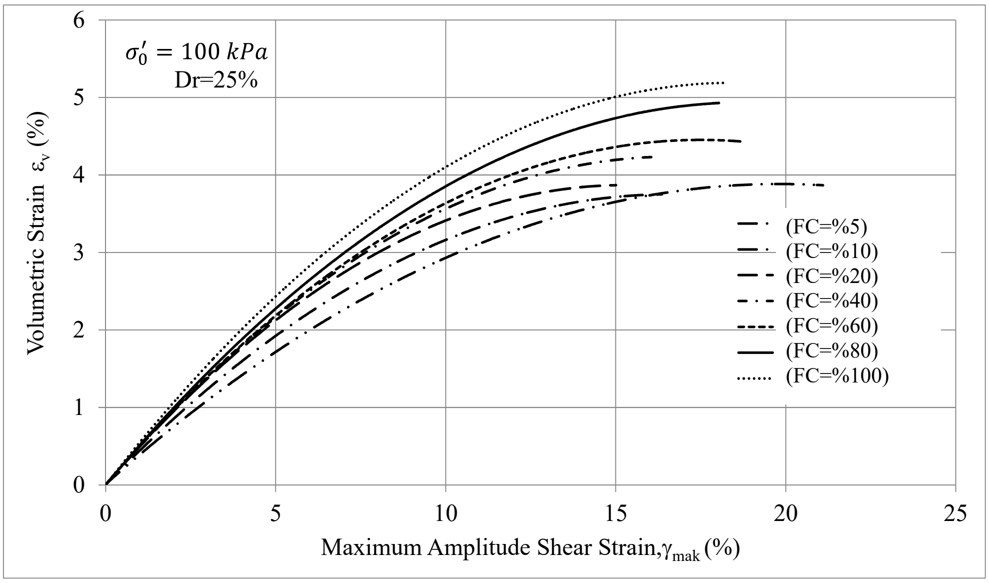

Figure 12. Correlation between the volumetric strain and maximum amplitude of shear strain *of samples with a relative density of Dr=25%*

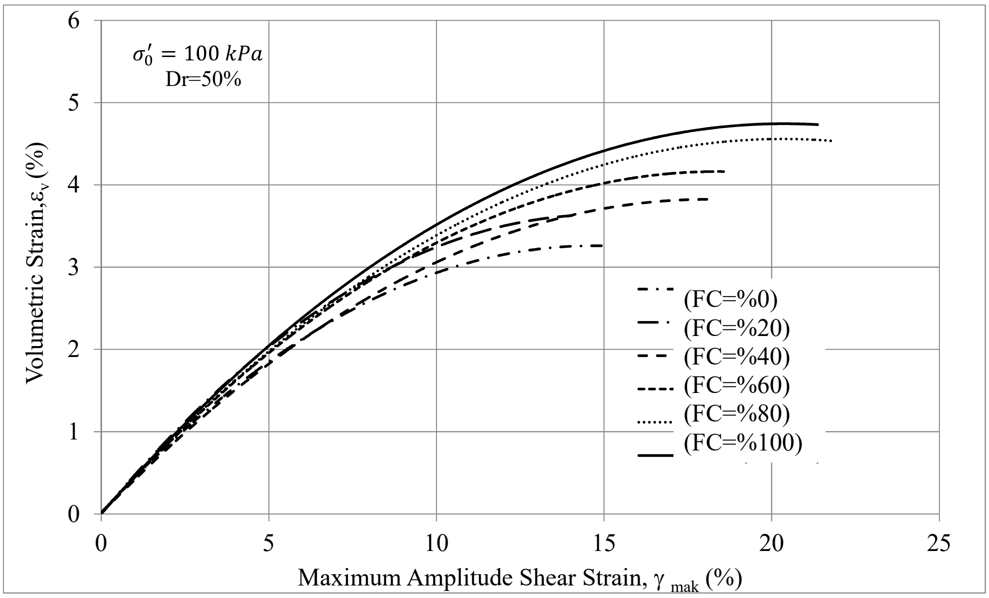

Figure 13. Correlation between the volumetric strain and maximum amplitude of shear strain *of samples with a relative density of Dr=50%*

In this study a relationship between the volumetric strain and maximum amplitude of shear strain was determined as follows:

$$\varepsilon_v = \log\,(a + b * \gamma_{mak}) \tag{3}$$

Here, it was seen that parameters a and b changed depending on the silt content. The change of parameters a and b according to two different relative densities and Eight different silt contents are shown with their determination coefficients in Tables 3 and 4. As a result of regression analyses, it was seen that the determination coefficient (R^2) obtained for parameters a and b were higher than 0.95. The parameter a was determined about 1 irrespective of the silt content. It was seen that parameter b was silt content dependent. It was determined that parameter b was about 3 if the silt content was zero (FC=%0) and value b took the value of approximately 10 as the silt content increased to 100% (FC=%100).

Table 3. Volumetric strain and maximum amplitude of shear strain for Dr=25%

Silt Content (F.C)	a	b	Determination Coefficient (R^2)	Sum Squares of Residuals
0	1.0031	3.0456	0.9751	0.2798
5	1.0026	2.5905	0.9697	0.3481
10	1.0061	2.3529	0.9525	0.5481
20	1.0005	3.1696	0.9991	0.0087
40	1.0008	4.2507	0.9812	0.2582
60	1.0022	4.6580	0.9659	0.50631
80	1.0005	7.6152	0.9811	0.3551
100	1.0007	9.8097	0.9698	0.6239

Table 4. Volumetric strain and maximum amplitude of shear strain for Dr=50%

Silt Content (F.C)	a	b	Determination Coefficient (R^2)	Sum Squares of Residuals
0	1.0148	1.6566	0.9367	0.4268
20	1.0014	2.6338	0.9894	0.1038
40	1.0041	2.4749	0.9783	0.2222
60	1.0024	3.4514	0.9858	0.1824
80	1.0009	3.4507	0.9976	0.0299
100	1.0005	5.3346	0.9881	0.1915

3.3. Correlation between Maximum Amplitude of Shear Strain and Factor of Safety for Silty Sands

In order to estimate the settlement after the liquefaction of soils, it is necessary to know maximum amplitude of shear strain that occurred during the earthquake. The cyclic resistance, is defined as the condition where effective confining stress is equal to the pore water pressure when a specific level of shear strain is achieved. This case may be defined as the initiation of liquefaction or development of 100% pore water pressure. In the laboratory, this procedure corresponds to the double amplitude of axial strain of 5% or it corresponds to 20 cycles. Consequently, the factor of safety defined in liquefaction studies is as follows;

$$G_s = \frac{\tau_{dev,L}}{\tau_{dev}} = \frac{\left(\sigma_{dl}/2\sigma_0'\right)_{20}}{\left(\sigma_d/2\sigma_0'\right)_{20}} = \frac{CSR_L}{CSR} \tag{4}$$

Here, CSR_L is CSR value which corresponds to 20 cycles required for liquefaction. In equation 4, σ_{dl} indicates the required axial strain which leads to liquefaction or the axial strain at 5% double amplitude for 20 cycles and σ_d indicates the earthquake dependent shear stress due to the progress of axial strain amplitude. In the above equation, if factor of safety is one it indicates that double amplitude of axial strain of 5% is achieved by cyclic softening and if the factor of safety was smaller than one indicates double amplitude of axial strain lower than 5% caused the softening of the soil . Therefore, the factor of safety is assessed as a function of double amplitude of axial strain and if the factor of safety in a region is known development of double amplitude of axial strain during liquefaction may be predicted. It is accepted that single amplitude of axial strain is the maximum shear strain that the soil is subjected to during liquefaction.

In the experiments conducted on silt sand mixtures at two different relative densities (Dr=25% and Dr=50%), the axial strain results at maximum amplitude corresponding to the factor of safety are shown in Figures 14 and 15. In the figures, it was seen that the shear strain increased as the silt content increased both for samples with relative densities of Dr=25% and Dr=50%. Therefore, it was observed that the silt content increment resulted in higher shear strain levels.

As a result of these experiments, a correlation was developed;

$$G_s = \frac{\gamma_{mak}}{(a + b * \gamma_{mak} + c * \sqrt{\gamma_{mak}})} \tag{5}$$

Equation (5) is a function of the factor of safety and shear strain at maximum amplitude. Here, it was seen that a, b and c parameters changed depending of the silt content (FC). The change of a, b and c parameters in accordance with two different relative densities and eight different silt contents are shown in Table 5 along with the determination coefficients. As a result of the regression analyses, it was seen that the determination coefficient obtained for a, b and c parameters (R^2) was higher than 0.92.

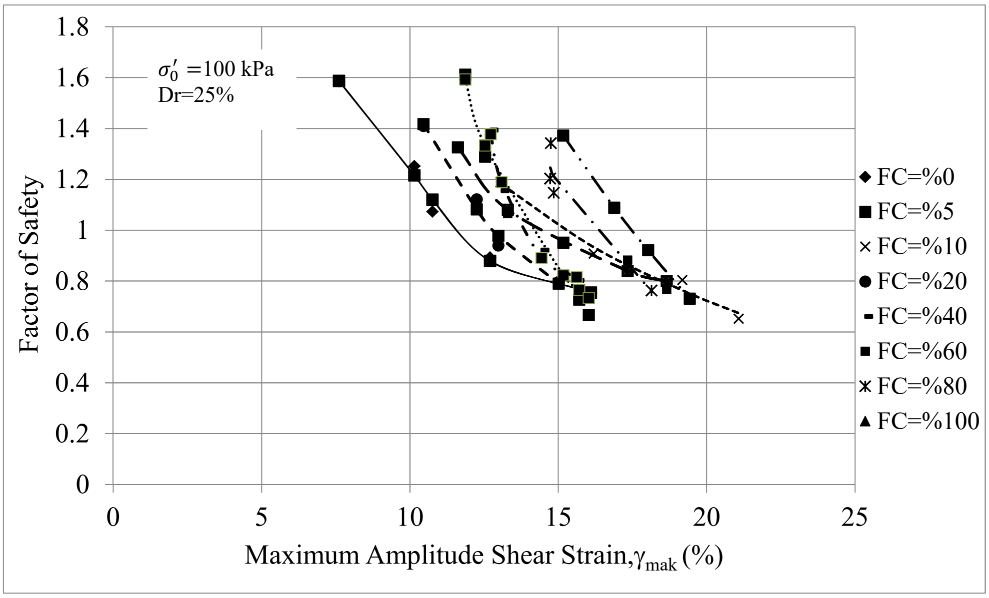

Figure 14. Safety factor and axial strain results at maximum amplitude *for Dr=25%*

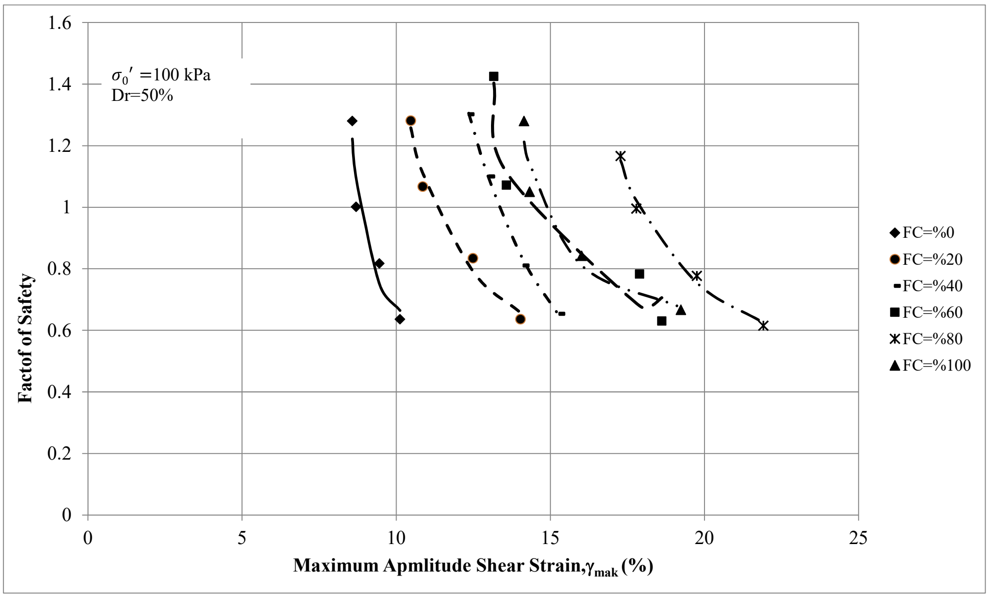

Figure 15. Safety factor and axial strain results at maximum amplitude for Dr=50%

Table 5. Safety factor and shear strain coefficients at maximum amplitude for Dr=50%

Silt Content (FC)	a	b	c	Determination Coefficient (R^2)	Sum Squares of Residuals
0	-583.247	-53.1311	357.1486	0.9237	0.0172
20	-42.4158	2.632625	7.159983	0.9800	0.0046
40	312.1531	31.19776	-195.77	0.9983	0.0004
60	-716.301	-40.6086	347.3401	0.9490	0.0187
80	-189.093	-2.30841	58.69417	0.9916	0.0014
100	-373,164	-17.1754	166.9142	0.9349	0.0136

3.4. Correlation between Factor of Safety and Volumetric Strain for Silty Sands

In the liquefaction analyses held by the traditional methods, determining the shear strain at maximum amplitude is not necessarily needed if the factor of safety is known and the post-liquefaction volumetric strain may be directly estimated. Within the scope of this study, the volumetric strain versus the factor of safety for the samples having different silt contents and relative densities were obtained and graphed in Figures 16 and 17. Here, it was shown that volumetric strain values did not change for two different relative densities for the samples with the same silt content. It was observed that the factor of safety varied between 0.6 and 1.6 cyclic stress ratio (CSR)depending on the samples having the same silt content and consolidated under the same effective confining stresses. Large deformation values were obtained as the samples were subjected to cyclic loading until the sample collapsed and it was observed that the values of volumetric strain were very close to each other between the observed factor of safety range. For example; if the experiments no. 1 and 2 in Table 2 are compared, cyclic stress ratio (CSR) values were 0.156 and 0.222, respectively. The factor of safety obtained depending on the CSR values were between 1.073 and 0.753, respectively. However, the volumetric strain values at the end of experiment were between 3.198 and 3.188, respectively. The difference between the volumetric strain values was only 0.01%. Therefore, similar volumetric strain values were obtained in the experiments which have different CSR values for the samples having the same silt contents. In Figures 16 and 17, it is shown that the volumetric strains were close to each other at a specific factor of safety range for the samples having the same silt contents.

It was also observed that the increase in the silt content also increased the strain values. As a comparison, the experiment sets no. 1 and 31 were discussed. The silt content was (FC=%0) and cyclic stress ratio was (CSR=0.156) in experiment no. 1. In experiment no. 31, the silt content (FC=%100) and cyclic stress ratio (CSR=0.156) had the same values with the experiment no. 1. It is seen that volumetric strain values were 3.198% and 4.978%, respectively for the experiments no. 1 and 31. A difference of 1.780% was achieved among the volumetric strain values. This condition showed that the water retention capacities of fine particles increased as the silt content increased in the soil and greater water discharge occurred by opening the drain valves at the end of loading and caused larger volumetric changes. Figure 16 and 17 point out that if the fines content increase and the soil type changes from clean sands to pure silts volumetric strain levels are increased regardless of the relative densities considered in this study.

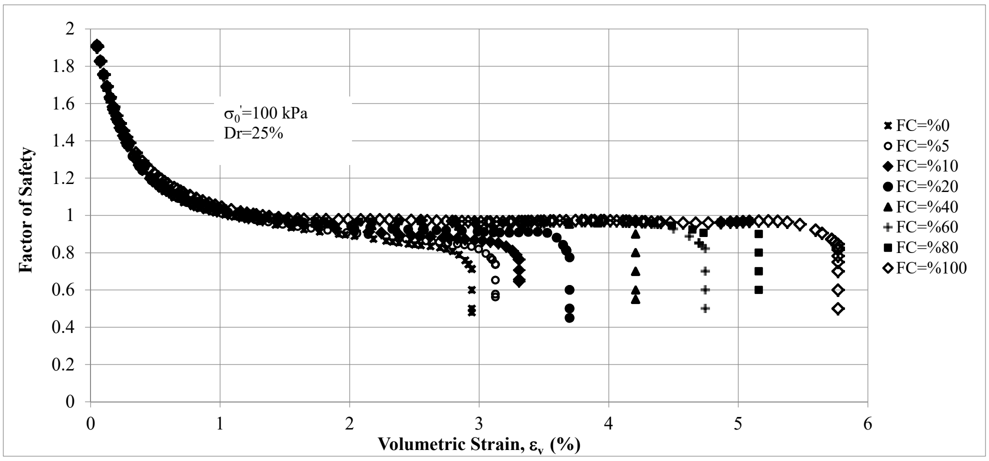

Figure 16. Correlation of safety factor and volumetric deformation for Dr=25%

The relationship between the factor of safety and volumetric strain for samples having the same silt contents and different relative densities (Dr=25% and Dr=50%) are shown in Figures 18 and 19. Figure 18 shows the relationship of factor of safety with volumetric strain for a clean sand and Figure 19 shows the relationship of factor of safety with volumetric strain for pure silt soil. It was observed that the volumetric strain values decreased as the relative density increased for each silt content. This conclusion is in conformity with the literature.

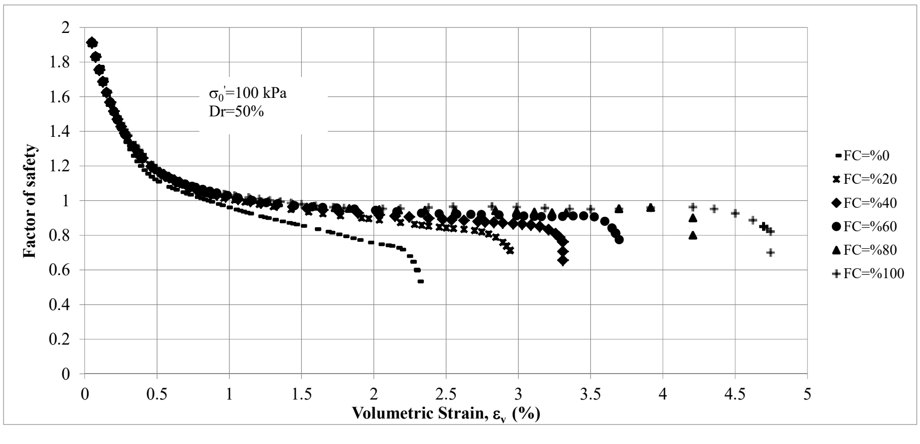

Figure 17. Correlation of safety factor and volumetric deformation for Dr=50%

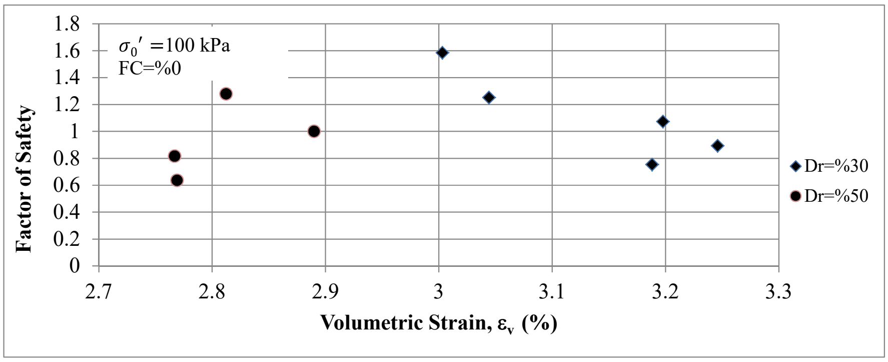

Figure 18. Correlation of safety factor and volumetric deformation for FC=0%

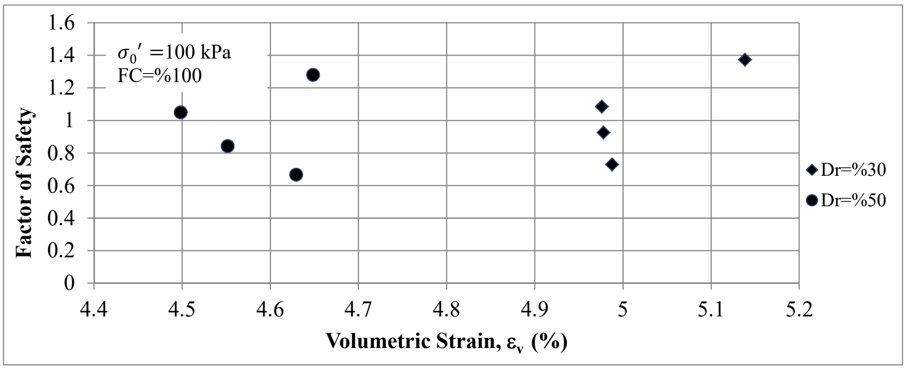

Figure 19. Correlation of safety factor and volumetric deformation for FC=100%

4. RESULTS

The results of this study were interpreted with the conceptual framework suggested by Theveyanagam [10] in terms of intergranular and interfine void ratios. Therefore, it offers a satisfactory level of interpretation for the parameters offered within the scope of this study and the behavior of the silt-sand mixtures under dynamic loadings becomes predictable.

Under constant effective confining stress, both intergranular void ratio and interfine void ratio were obtained with the cyclic stress ratio (CSR_{20}) corresponding to 20 cycles. According to the experiment results, the threshold silt content value was found as 40%. For every mixture tested, it was observed that CSR_{20} value decreased for increasing values of intergranular or interfine void ratios. However, CSR_{20} value would also increase if the silt content increased up to the threshold silt content for a given intergranular void ratio. As the silt content increases, the decrease at CSR_{20} value is shown by means of the interfine void ratio. For a constant intergranular void ratio, the void ratio of the mixture decreases as the silt content increases and therefore the soil mixture becomes more resistant to the dynamic effects. On the contrary, for a given interfine void ratio, if the silt content exceeds the threshold value the void ratio of this mixture increases and the soil becomes less resistant to the dynamic effects. The experimental results of this study also show that there is a general consensus with the findings of literature concerning the effect of silt content on the liquefaction behavior of silt sand mixtures.

It was observed that the volumetric strain values increased as the silt content increased for the maximum amplitude of shear strain which was taken as a constant for both relative densities of this study. A logarithmic correlation between the volumetric strain and the maximum amplitude of shear strain was also obtained. In this equation, it was determined that b value increased with the silt content of silt sand mixtures.

References

[1] Seed, H. B., and Lee K. L, "Liquefaction of Saturated Sands during cyclic Loading" J. Soil Mech. And found. Div., ASCE 92 (6), p105-134, 1966.

[2] Seed HB, Tokimatsu K, Harder LF, Chung RM. Influence of SPT procedures in soil liquefaction resistance evaluations. J Geotech Eng, ASCE;111(12) p1425–45, 1985.

[3] Koester JP. In: Prakash S, Dakoulas P, editors. The influence of fines type and content on cyclic strength. Ground failures under seismic conditions, 44. ASCE Publication; p. 17–33, 1994.

[4] Troncoso, J.H. "Failure Risks of Abandoned Tailings Dams" Proc. Int. Sym. On Safety and Rehabilitation of Tailings Dams, International Commission on Large Dams, Paris, p82-89, 1990.

[5] Ishihara. Soil behaviour in earthquake geotechnics. Oxford Engng Sci Ser 1993;46.

[6] Guo, T. and Prakash, S., Liquefaction of Silts and Silt-Clay Mixtures", Journal of Geotechnical and Geoenvironmental Engineering, ASCE, Vol. 125, No. 8, p706-710. 1999.

[7] Finn LWD, Ledbetter RH, Guoxi WU. Liquefaction in silty soils: design and analysis. In: Prakash S, Dakoulas P, editors. Ground failures under seismic conditions. ASCE Geotechnical Special Publication, vol. 44, p. 51–76, 1994.

[8] Polito, C. P., and Martin II, J. R. Effects of non-plastic fines on the liquefaction resistance of sands. Journal of Geotechnical and Geoenvironmental Engineering, 127, p408–415, 2001.

[9] Thevanayagam, S. Effect of fines and confining stress on undrained shear strength of silty sands. Journal of Geotechnical and Geoenvironmental Engineering, 124, p479–491. 1998.

[10] Thevanayagam, S. and Mohan, S. Intergranular state variables and stress strain behavior of silt sand, Geotechnique 50(1),p1-23, 2000.

[11] Vaid YP. Liquefaction of silty soils. In: Prakash S, Dakoulas P, editors. Ground failures under seismic conditions, 44. ASCE Publication;. p. 1–16, 1994.

[12] Amini, F., and Qi, G. Z. Liquefaction testing of stratified silty sands. Journal of Geotechnical and Geoenvironmental Engineering, 126, p208–217, 2000.

[13] Belkhatir, M., Arab, A., Della, N., Missoum, H., & Schanz, T. Liquefaction resistance of Chlef river silty sand: Effect of low plastic fines and other parameters. Acta Polytechnica Hungarica, 7, p119–137, 2010.

[14] Stamatopoulos, C. An experimental study of the liquefaction strength of silty sands in terms of the state parameter. Soil Dynamics and Earthquake Engineering, 30, p662–678 2010.

[15] Papadopoulou, A., and Tika, T. The effect of fines on critical state and liquefaction resistance characteristics of non-plastic silty sands. Soils and Foundations, 48, p713–725, 2008.

[16] Xenaki, V. C., and Athanasopoulos, G. A. Liquefaction resistance of sand-silt mixtures: An experimental investigation of the effect of fines. Soil Dynamics and Earthquake Engineering, 23, p183–194, 2003.

[17] Polito CP. The effects of non-plastic and plastic fines on the liquefaction of sandy soils. PhD Thesis, Virginia Polytechnic Institute and State University, Blacksburg. 1999.

[18] Monkul, M. M., Ozden, G. “Effect of intergranular void ratio on one-dimensional compression behavior”. GEOPROB 2005:Proceedings of International Conference on Problematic Soils, International Society of Soil Mechanics and Geotechnical Engineering (ISSMGE), Famagusta, KKTC, 3, p1203-1209, 2005.

[19] Yang, S. L., Lacasse, S., and Sandven, R. (Determination of the transitional fines content of mixtures of sand and non-plastic fines. Geotechnical Testing Journal, 29, p102–10, 2006.

[20] Kuerbis, R. H., Negussey, D., and Vaid, Y. PEffect of gradation and fines content on the undrained response of sand. In D. J. A. Van Zyl (Ed.), Fort Collins, CO: Geotechnical Special Publications Hydraulic fill structures. p. 330–345, 1988.

[21] Dash, H. K., and Sitharam, T. G. Undrained monotonic response of sand-silt mixtures:Effect of nonplastic fines. Geomechanics and Geoengineering, 6, p47–58. 2011.

[22] Dasari, G. R., Ni, Q., Tan, T. S., and Hight, D. W. Contribution of fines to the compressive strength of mixed soils. Géotechnique, 54, p561–569, 2004.

[23] Lee, K., and Albaisa, A., Earthquake Induced Settlement in Saturated Sands. ASCE Journal of Geotechnical Engineering Divisions (100), p.387-406, 1974.

[24] Tatsuoka, F., Muramatsu M. and Sasaki T., Cyclic undrained stress-strain behavior of dense sands by torsional simple shear test, Soils and Foundations, 22, p.55-70, 1982.

[25] Ishihara, K., Tatsuoka, F., and Yasuda, S., Effects of Overconsolidated Sand and Liquefaction Characteristic of Sands Containings Fines. Dynamic Geotechnical Testing (654), p.246-264, 1978.

[26] Tokimatsu, K. and H.B. Seed, Evaluation of settlements in sands due to earthquake shaking, J. Geot. Engrg., 113 (8), p861-878, 1987.

[27] Ishihara, K. and Yoshimine, M.. Evaluation of settlements in sand deposits following liquefaction during earthquakes. Soils and Foundations. Vol. 32(1): p173-188, 1992.

[28] Tatsuoka, F., Muramatsu M. and Sasaki T.,. Cyclic undrained stress-strain behavior of dense sands by torsional simple shear test, Soils and Foundations, 22, p.55-70, 1982.

[29] Kondoh, M., Sasaki, Y. and Matsumoto, H. Effects of fines contents on soil liquefaction strength, Proceedings Annual Meeting of the Japanese Society of Soil Mechanics and Foundation Engineering, Tsukuba,Japan 1987.

[30] Kokusho, T., Yoshida, Y., Nishi, K. and Esashi, Y. Evaluation of Seismic Stability of Sand Layer (Part I) Report 383025, Electric Power Central Research Institute. 1983.